Chinese Chemical Letters 34 (2023) 108029

Contents lists available at ScienceDirect

Chinese Chemical Letters

journal homepage: www.elsevier.com/locate/cclet

Photocatalytic Cr(VI) reduction over MIL-88A(Fe) on polyurethane sponge: From batch to continuous-flow operation

Xiao-Hong Yi[a,b], Ya Gao[a,b], Chong-Chen Wang[a,b,*], Yu-Hang Li[a,b], Hong-Yu Chu[a,b], Peng Wang[a,b]

[a] Beijing Key Laboratory of Functional Materials for Building Structure and Environment Remediation, School of Environment and Energy Engineering, Beijing University of Civil Engineering and Architecture, Beijing 100044, China
[b] Beijing Energy Conservation & Sustainable Urban and Rural Development Provincial and Ministry Co-construction Collaboration Innovation Center, Beijing University of Civil Engineering and Architecture, Beijing 100044, China

ARTICLE INFO

Article history:
Received 6 September 2022
Revised 14 November 2022
Accepted 28 November 2022
Available online 30 November 2022

Keywords:
MIL-88A(Fe)
Polyurethane sponge
Cr(VI) reduction
Tartaric acid
Continuous operation

ABSTRACT

MIL-88A(Fe)@sponge (MS) was synthesized by a dip-coating method, which displayed efficient photocatalytic Cr(VI) reduction efficiency under both low power LED UV light and real solar light irradiation. It was observed that MS (0.2 g/L) could remove 100% Cr(VI) (10 mg/L) by adding 0.4 mmol/L tartaric acid (TA) without adjusting pH (pH 5.05) within 6.0 min and 3.0 min under UV light and real solar light irradiation, respectively. Besides, the photo-induced e^- and radicals ($O_2^{\bullet-}$ and $CO_2^{\bullet-}$) were found to play the momentous roles in the MS/TA/UVL/Cr(VI) system by the scavenger experiments and electron spin resonance (ESR) tests. MS was also filled into a fixed-bed reactor to test the possibility of long-term Cr(VI) reduction operation in TA/UVL system. As expected, the results revealed that MS could still maintain 100% activity up to 60 h. These results demonstrated that MIL-88A(Fe) might be the potentially efficient catalyst for large-scale wastewater treatment in the near future.

Water pollution, as one of the most urgent problems in the world, has caused irreparable damage to the environment and human health [1]. Generally, wastewater contains various kinds of pollutants, such as oils, organic pollutants, and heavy metal ions [2–4]. Chromium is a typical heavy metal element in the environment, which has caused extensive concern because of its toxicity, non-biodegradability and durability [5]. Cr(VI) as the most toxic form of Chromium, might lead to carcinogenicity and mutagenicity to organisms [5,6]. Compared with Cr(VI), Cr(III) is an essential nutrient and easy to precipitate [5,6].

The advanced reduction process (ARP) has attracted more and more attention due to its ability to remove oxidative pollutants from wastewater [7]. Carboxyl anionic radicals ($CO_2^{\bullet-}$) are common reducing intermediates in wastewater treatment [8]. Although the reducibility is relatively weak compared with electrons (e^-) [9], it is easier to generate $CO_2^{\bullet-}$ through the electron transfer between small molecular carboxylic acids (SMCAs) (such as malic, malonic, formic, oxalic, tartaric, citric acid) and catalysts in the photocatalysis [10]. In addition, these SMCAs are nontoxic and easily mineralized, and they can inhibit the recombination of photogenerated e^--h^+ pairs and thus induce the photocatalytic reduction of Cr(VI) when they are used for eliminating the holes [10]. Therefore, it is very important to develop functional materials to remove Cr(VI) from water through the ARP.

Metal-organic frameworks (MOFs) have been extensively utilized in the field of water pollution remediation owing to its adjustable structure, large porosity and specific surface area and so on [11]. Nevertheless, the application of MOF powders in large-scale water pollution remediation has been greatly limited, such as its easy agglomeration, difficult separation and recovery [12]. In our previous studies, the UiO-66-NH_2(Zr/Hf) and MIL-101(Fe)-NH_2 were fabricated on the α-Al_2O_3 substrate to reduce Cr(VI) to Cr(III) under white light irradiation [13,14], in which MIL-101(Fe)-NH_2@α-Al_2O_3 was used for continuous treatment of wastewater due to its characteristics of easy recovery and recycling. Here, a facile, cheap and easy-to-use method was adopted to immobilize MIL-88A(Fe) onto three-dimensional macroporous polyurethane sponge to obtain MIL-88A(Fe)@sponge (MS) with the aid of polyvinyl butyral (PVB) as adhesive agent.

Analytical grade reagents and chemicals were utilized in the studies with no additional purification. And the detailed information of the chemicals and characterization methods was shown in

* Corresponding author at: Beijing Key Laboratory of Functional Materials for Building Structure and Environment Remediation, School of Environment and Energy Engineering, Beijing University of Civil Engineering and Architecture, Beijing 100044, China.
E-mail address: wangchongchen@bucea.edu.cn (C.-C. Wang).

https://doi.org/10.1016/j.cclet.2022.108029
1001-8417/

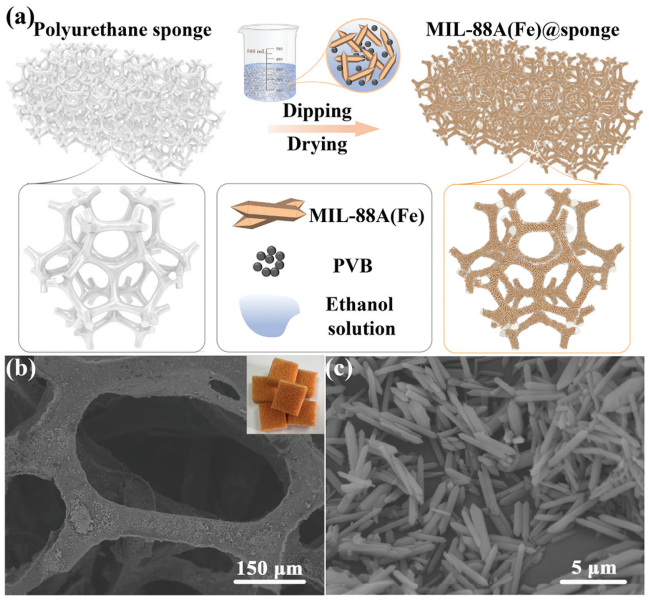

Fig. 1. (a) The preparation procedure of MS. (b, c) SEM images of MS (Inset: the photograph of MS).

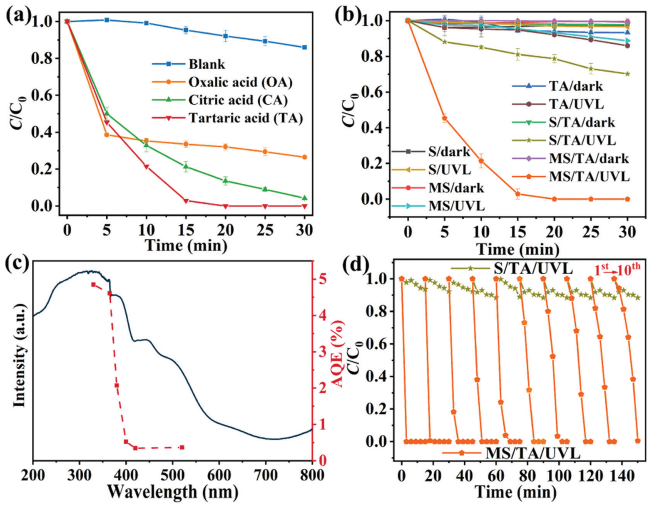

Fig. 2. The Cr(VI) removal efficiencies over MS under LED UV light irradiation. (a) Effects of different small molecular acids. Reaction conditions: MIL-88A(Fe) = 10.0 mg, volume = 50.0 mL, $[Cr(VI)]_0 = 10.0$ mg/L, $[TA]_0 = [CA]_0 = [OA]_0 = 0.2$ mmol/L, pH 2.00. (b) Comparison of different experimental conditions. Reaction conditions: MIL-88A(Fe) = 10.0 mg, volume = 50.0 mL, $[Cr(VI)]_0 = 10.0$ mg/L, [TA] = 0.2 mmol/L, pH 2.00. (c) AQEs of Cr(VI) reduction over MS in the presence of TA. (d) Reusability test of MS. Reaction conditions: MIL-88A(Fe) = 10.0 mg, volume = 50.0 mL, $[Cr(VI)]_0 = 10.0$ mg/L, [TA] = 0.4 mmol/L, unadjusted pH 5.05.

Supporting information (Texts S1 and S2 in Supporting information).

According to the previous report, the rod-like MIL-88A(Fe) was synthesized by hydrothermal method (Text S3 in Supporting information) [15]. And the synthesis process of MS is schematically illustrated in Fig. 1a (The detailed preparation procedure can be seen in Text S3 in Supporting information). Fig. S2 (Supporting information) shows that the surface and skeleton of the initial polyurethane sponge with plenty of porous in different sizes was clean and smooth. After the immobilization of MIL-88A(Fe), the surface of the skeleton became rough and covered by rod-like MIL-88A(Fe) film with the particle size of 2–6 μm (Figs. 1b and c). Besides, the uniform distribution of the target elements (Fe, C and O) of MIL-88A(Fe) was observed in the EDS-mapping analysis (Fig. S3 in Supporting information).

The photocatalytic Cr(VI) reduction over MS under LED UV light (UVL) in the presence of oxalic acid (OA), citric acid (CA) and tartaric acid (TA) were carried out to evaluate the catalytic performance of different small molecular acid. As presented in Fig. 2a, the Cr(VI) reduction efficiencies decreased in the presence of TA (100%) > CA (86.4%) > OA (67.9%) > blank (7.9%), which can be contributed to the decreasing number of α-hydroxyl groups [16]. TA was used to enhance the photocatalytic Cr(VI) reduction in the following experiments. The Cr(VI) elimination efficiencies within 20.0 min were negligible in the S/dark (0.5%), MS/dark (2.8%), TA/dark (0.2%), S/TA/dark (2.0%), MS/TA/dark (6.0%), S/UVL (3.1%), MS/UVL (6.7%) and TA/UVL (7.9%) systems (Fig. 2b), suggesting that the above mentioned processes are unreactive toward Cr(VI). Under LED UV light irradiation, only 21.3% Cr(VI) was reduced over bare sponge in the presence of TA for 20.0 min. In contrast, in MS/TA/UVL system, 100% Cr(VI) was reduced after being irradiated for 20.0 min, suggesting that the introduction of MIL-88A(Fe) enhanced the photocatalytic Cr(VI) reduction.

Further, the apparent quantum efficiencies (AQEs) of Cr(VI) reduction over MS within 1.5 min under different light absorption spectra were also calculated, which is an important metric for evaluating the operational efficiency of the photocatalytic system. As depicted in Fig. 2c, the AQEs over MS were 4.84%, 4.61%, 2.07%, 0.52%, 0.37% and 0.35% at $\lambda = 330$ nm, 365 nm, 380 nm, 400 nm, 420 nm and 520 nm, respectively. The results of the one-to-one mapping between the AQE and the light adsorption spectrum suggested that the reaction proceeds through photoinduced process [8].

It can be observed that the Cr(VI) reduction efficiency accelerated with the increasing concentrations of TA (Fig. S7a in Supporting information). The elimination efficiency of Cr(VI) increased dramatically from 33.2% to 100% as the starting concentration of TA was increased from 0.1 mmol/L to 0.8 mmol/L within 5.0 min, and the k value was increased 11.8-fold (Fig. S7b in Supporting information). The increasing TA concentration could induce to yield more active species for promoting the Cr(VI) reduction efficiency [10]. Zhu *et al.* also discovered that higher SMCAs concentration caused faster Cr(VI) reduction [10]. The optimal TA concentration was selected as 0.4 mmol/L in the MS/TA/UVL/Cr(VI) system considering both the operation cost and the efficiency.

As illustrated in Fig. S7c (Supporting information), it was worth to noting that the pH alteration exerted ignorable impact on the Cr(VI) reduction degree, because the introduced TA can be ionized to release H^+ for retaining low pH [17]. Specifically, the pH of the solution dropped from 2.04, 3.04, 4.02, 5.05, 5.98, 7.99, 9.95 to 2.00, 3.00, 3.39, 3.45, 3.55, 3.73 and 3.85, respectively (Fig. S7c inset). However, the solution pH increased to 2.04, 3.23, 4.12, 4.32, 4.52, 4.64 and 4.98 with the end of the reaction, due to that TA and H^+ could be consumed during the reaction [17].

Furthermore, the photoreduction capacity of MS has also been investigated in the presence of a variety of interfering inorganic anions in order to better understand its practical applications. As depicted in Fig. S7d (Supporting information), no significant effect of HCO_3^- was observed, and the inorganic anions such as Cl^-, NO_3^-, SO_4^{2-}, $H_2PO_4^-$ exhibited a minimal decrease in the reduction efficiency of MS. It might be attributed to the adsorption competition between above-mentioned anions and Cr(VI), which led to the declined capture of Cr(VI) and significant decrease of photocatalytic efficiency [18]. To study the practical application of the MS, the real tap water and lake water were also selected to prepare Cr(VI) solutions for photocatalytic reactions [16]. As it can be observed in Fig. S7e (Supporting information), the reduction efficiencies of Cr(VI) in the simulated aqueous solutions from lake water

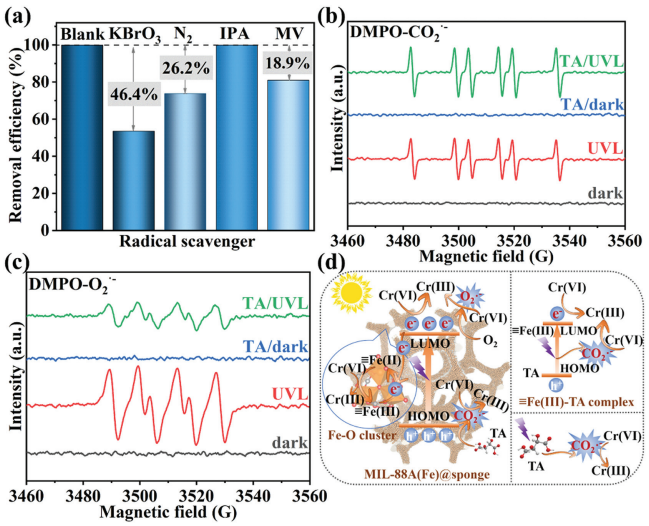

Fig. 3. (a) Effect of $KBrO_3$, N_2, IPA and MV on Cr(VI) reduction over MS. Reaction conditions: MIL-88A(Fe) = 10.0 mg, volume = 50.0 mL, $[Cr(VI)]_0 = 10.0$ mg/L, $[TA]_0 = 0.4$ mmol/L, $[KBrO_3]_0 = [IPA]_0 = [MV]_0 = 20$ mmol/L, unadjusted pH 5.05. The ESR spectra of (b) DMPO-$CO_2^{\bullet-}$ and (c) DMPO-$O_2^{\bullet-}$ over MS. (d) The possible mechanism of Cr(VI) reduction over MS with the aid of TA under LED-UV light irradiation.

(78.6%) and tap water (72.1%) were lower than that in the pure water simulated solution. Fortunately, the 100% Cr(VI) reduction efficiencies could be accomplished if the reaction time was extended to 25.0 min. It can also be found that MS can remove Cr(VI) effectively with the aid of the TA under real solar light, indicating that MS has the potential to use actual solar energy directly (Fig. S7f in Supporting information). Table S1 (Supporting information) summarized an overview of publications published on typical catalysts for the Cr(VI) reduction with the aid of SMCAs, in which MS exhibited greater activity than those of its counterpart catalysts.

The exploration of stability and reusability of photocatalysts is very important to judge whether they can be used in practical applications. As depicted in Fig. 2d, there was no significant decrease of photocatalytic efficiency even after 10 runs, indicating that the MS had excellent reusability. Moreover, the reusability test of the MIL-88A(Fe) powder (M/TA/UVL) shown in Fig. S8 (Supporting information) exhibited that the MIL-88A(Fe) powder is unstable, since the catalytic performance exhibited a significant decrease in the 2nd cycle. The leaching Fe contents from MS/TA/UVL/Cr(VI) and M/TA/UVL/Cr(VI) system had been determined as 0.92 mg/L and 3.59 mg/L using an ICP-OES, respectively. Obviously, immobilizing MIL-88A(Fe) onto three-dimensional macroporous polyurethane sponge through the adhesion of PVB can significantly reduce Fe leaching and enhance its water stability. And, it was found that the structure and morphology of MS (Fig. S9 in Supporting information) were not significantly changed after 10 cycles, revealing the stability of MS.

The photo-induced e^- could directly reduce Cr(VI), as well as other reactive oxygen species could participate in the photocatalytic reaction process [8,14]. Herein, $KBrO_3$, isopropyl alcohol (IPA), methyl violet (MV) was used to capture e^-, $^{\bullet}OH$ and $CO_2^{\bullet-}$. Meanwhile, the introduction of N_2 was to eliminate dissolved oxygen in the solution to determine the role of the $O_2^{\bullet-}$. As depicted in Fig. 3a, about 46.4%, 26.2% and 18.9% suppression could be observed when $KBrO_3$, N_2 and MV were added to the MS/TA/UVL system, respectively, indicating that e^- played a leading role in the Cr(VI) photoreduction. In addition, $O_2^{\bullet-}$ and $CO_2^{\bullet-}$ were also related to the Cr(VI) reduction. Moreover, $^{\bullet}OH$ is not responsible for the Cr(VI) reduction, because MS can still reduce 100% of Cr(VI) after IPA was added to the MS/TA/UVL system.

ESR investigations were also conducted to investigate the role played by radical species in the MS/TA/UVL system. Obviously, the significant signals of DMPO-$CO_2^{\bullet-}$ [8] and DMPO-$O_2^{\bullet-}$ [19] can be observed in MS/TA/UVL system in Figs. 3b and c, confirming that $CO_2^{\bullet-}$ and $O_2^{\bullet-}$ played vital roles in the reduction of Cr(VI). In addition, Fig. 3b demonstrates that $CO_2^{\bullet-}$ radicals exist in the MS/UVL system, indicating that the UV light could excite the slightly dissolved fumaric acid from MIL-88A(Fe) to produce $CO_2^{\bullet-}$ [20]. As well, the signals of DMPO-$O_2^{\bullet-}$ were detected when the MS was excited by UV light (Fig. 3c), further affirming that $O_2^{\bullet-}$ was really produced during photocatalysis reaction.

In addition, the transfer and separation performance of photogenerated carriers were further confirmed by photocurrent and EIS measurements (Fig. S10 in Supporting information). Obviously, the MIL-88A(Fe)/TA/UVL system displayed an improvement in photocurrent response and a smaller Nyquist arc radius compared with other systems, indicating that the addition of TA might accelerate the charge transfer [21].

As mentioned above, the possible Cr(VI) reduction mechanism over the MS/TA/UVL system can be assumed in Fig. 3d. When being irradiated with UV light, MS generates e^- and h^+ [12]. Subsequently, the Cr(VI) was reduced to Cr(III) by e^- [14,16]. Otherwise, $O_2^{\bullet-}$ were produced *via* the reaction between e^- and O_2 [16] to reduce Cr(VI) [8]. Furthermore, e^- facilitates the *in situ* redox reaction between Fe(II) and Fe(III) in Fe-O cluster of MIL-88A(Fe) (Fig. S11 in Supporting information), thus accelerating the reduction of Cr(VI) [22]. Here, the addition of TA can significantly accelerate the performance of MS in reducing Cr(VI). Therefore, we summarized the following three aspects about the role of TA in reducing Cr(VI) in MS/TA/UVL/Cr(VI) system. Firstly, the electron transfer between MS and Cr(VI) could be greatly accelerated by the addition of TA because the TA can capture the h^+ generated by MS and generated the $CO_2^{\bullet-}$ to reduce Cr(VI) [17]. Secondly, TA might coordinate with the transition metals in both surface-bound/dissolved species to form both surface and aqueous Fe(III)-TA complexes [20]. And the high E_{HOMO} of TA could create a significant energy gap between the HOMO of TA and the LUMO of the Fe(III) ions, which could act as a stronger driving force for the e^- transfer between the TA ligand and the Fe(III) ions. The surface-bound and dissolved Fe(III)-TA complexes had been excited by UV light to accelerate the charge transfer from the TA to the Fe(III) ions, thus accelerating the electron reduction of Cr(VI) to Cr(III) [20]. As well, the formation of $CO_2^{\bullet-}$ was enhanced by the photoinduced electron transfer mechanism of the TA ligand and the Fe(III) ions [19]. Thirdly, UV light could excite the TA to produce $CO_2^{\bullet-}$, which could decrease the Cr(VI) to Cr(III) [20]. TA performed both the roles of electron donors and mediators in MS/TA/UVL system [20].

Due to the superior Cr(VI) reduction performance and cyclic stability of MS, we constructed a fixed-bed reactor to achieve continuous flow operation to purify the simulated wastewater containing Cr(VI) (Fig. 4 inset and Fig. S12 in Supporting information). As shown in Fig. 4, the individual UVL cannot reduce Cr(VI). The efficiency of the TA/UVL system for reducing Cr(VI) reached 52.9% at 3 h. Then, with the extension of time, its reduction efficiency decreased to 35.9%. The reduction efficiency of the S/TA/UVL system reached 80.1% at 3 h, and then it decreased continuously. In contrast, the reduction efficiency of the MS/TA/UVL system reached 100% up to 60 h, and the removal efficiency still reached more than 90% after 84 h. It was calculated that 1.0 kg MS can completely purify 93.1 t of wastewater with the Cr(VI) concentration of 10 mg/L within 60 h, in which the production cost of MIL-88A(Fe) is calculated as 2.788 CNY/g (Tables S2–S4 in Supporting information) based on the chemical and power input. The declining Cr(VI) reduction performance (Fig. 4) in the long-term operation can be as-

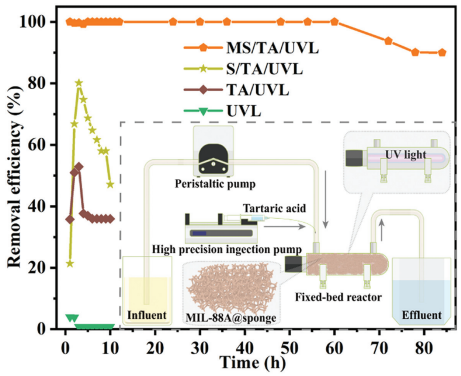

Fig. 4. Cr(VI) reduction efficiencies of different system under UV light irradiation during the long-term experiment (Inset: schematic diagram of self-assembled continuous operation reactor). Reaction conditions: MIL-88A(Fe) = 0.58 g, $[Cr(VI)]_0 = 10.0$ mg/L, 0.9 L/h, $[TA]_0 = 0.9$ mmol L^{-1} h^{-1}, HRT = 15.0 min, unadjusted pH 5.05.

cribed to the slow dissolution of the as-prepared MS, implying that more attempts should be performed to immobilize MIL-88A(Fe) for longer-term run.

In conclusion, the as-obtained 3D MIL-88A(Fe)@sponge displayed excellent catalytic performance in the reduction of toxic Cr(VI) with the help of tartaric acid under LED UV light irradiation. The e^- and radicals like $O_2^{\bullet-}$ and $CO_2^{\bullet-}$ played the major roles in the MS/TA/UVL/Cr(VI) system. More importantly, a fixed bed reactor was constructed to achieve continuous treatment of wastewater. This work further confirmed that MIL-88A(Fe)@sponge as an efficient and environmentally friendly catalyst possessed great potential in the continuous and long-term removal of pollutants in wastewater.

Declaration of competing interest

The authors declare that they have no known competing financial interests or personal relationships that could have appeared to influence the work reported in this paper.

Acknowledgments

This work was supported by National Natural Science Foundation of China (Nos. 22176012, 51878023), Beijing Natural Science Foundation (No. 8202016), Beijing Talent Project (No. 2020A27), and BUCEA Doctor Graduate Scientific Research Ability Improvement Project (No. DG2021004).

Supplementary materials

Supplementary material associated with this article can be found, in the online version, at doi:10.1016/j.cclet.2022.108029.

References

[1] R.P. Schwarzenbach, T. Egli, T.B. Hofstetter, U. von Gunten, B. Wehrli, Annu. Rev. Environ. Resour. 35 (2010) 109–136.
[2] M. Wang, H.S. Tsai, C. Zhang, C. Wang, S.H. Ho, Chin. Chem. Lett. 33 (2022) 2807–2816.
[3] Y. Dai, J. Yao, Y. Song, S. Wang, Y. Yuan, Environ. Sci.: Nano 3 (2016) 857–868.
[4] S.P. Wu, X.Z. Dai, J.R. Kan, F.D. Shilong, M.Y. Zhu, Chin. Chem. Lett. 28 (2017) 625–632.
[5] S. Prasad, K.K. Yadav, S. Kumar, et al., J. Environ. Manag. 285 (2021) 112174.
[6] C.C. Wang, X. Ren, P. Wang, C. Chang, Chemosphere 303 (2022) 134949.
[7] X. Liu, G. Liu, S. You, Chemosphere 263 (2021) 127898.
[8] Y.H. Li, X.H. Yi, Y.X. Li, et al., Environ. Res. 201 (2021) 111596.
[9] R. Flyunt, M.N. Schuchmann, C. von Sonntag, Chemistry 7 (2001) 796–799.
[10] C. Zhu, Y. Li, Y. Zhang, et al., Colloid. Surf. A 642 (2022) 128657.
[11] C.Y. Wang, L. Ma, C.C. Wang, et al., Environ. Funct. Mater. 1 (2022) 49–66.
[12] J.S. Wang, X.H. Yi, X. Xu, et al., Chem. Eng. J. 431 (2022) 133213.
[13] X.D. Du, X.H. Yi, P. Wang, et al., Chem. Eng. J. 356 (2019) 393–399.
[14] Q. Zhao, X.H. Yi, C.C. Wang, P. Wang, W. Zheng, Chem. Eng. J. 429 (2022) 132497.
[15] X. Liao, F. Wang, F. Wang, et al., Appl. Catal. B: Environ. 259 (2019) 118064.
[16] X.H. Yi, S.Q. Ma, X.D. Du, et al., Chem. Eng. J. 375 (2019) 121944.
[17] W. Yang, Z. Yang, L. Shao, et al., J. Environ. Sci. 107 (2021) 194–204.
[18] Y.X. Li, C.C. Wang, H. Fu, P. Wang, J. Environ. Chem. Eng. 9 (2021) 105451.
[19] J. Guo, J. Deng, B. An, et al., Chemosphere 295 (2022) 133785.
[20] B. Jiang, Y. Gong, J. Gao, et al., J. Hazard. Mater. 365 (2019) 205–226.
[21] Y. Zhang, Y. Dai, L. Yin, et al., Catal. Sci. Technol. 10 (2020) 3654–3663.
[22] W. Liao, Z. Ye, S. Yuan, et al., Environ. Sci. Technol. 53 (2019) 13767–13775.